Reversal of experimental pulmonary hypertension by PDGF inhibition

Ralph Theo Schermuly, Eva Dony, Hossein Ardeschir Ghofrani, Soni Pullamsetti, Rajkumar Savai, Markus Roth, Akylbek Sydykov, Ying Ju Lai, Norbert Weissmann, Werner Seeger, and Friedrich Grimminger

Department of Internal Medicine, Justus-Liebig-University Giessen, Giessen, Germany.

Progression of pulmonary hypertension is associated with increased proliferation and migration of pulmonary vascular smooth muscle cells. PDGF is a potent mitogen and involved in this process. We now report that the PDGF receptor antagonist STI571 (imatinib) reversed advanced pulmonary vascular disease in 2 animal models of pulmonary hypertension. In rats with monocrotaline-induced pulmonary hypertension, therapy with daily administration of STI571 was started 28 days after induction of the disease. A 2-week treatment resulted in 100% survival, compared with only 50% in sham-treated rats. The changes in RV pressure, measured continuously by telemetry, and right heart hypertrophy were reversed to near-normal levels. STI571 prevented phosphorylation of the PDGF receptor and suppressed activation of downstream signaling pathways. Similar results were obtained in chronically hypoxic mice, which were treated with STI571 after full establishment of pulmonary hypertension. Moreover, expression of the PDGF receptor was found to be significantly increased in lung tissue from pulmonary arterial hypertension patients compared with healthy donor lung tissue. We conclude that STI571 reverses vascular remodeling and cor pulmonale in severe experimental pulmonary hypertension regardless of the initiating stimulus. This regimen offers a unique novel approach for antiremodeling therapy in progressed pulmonary hypertension.

Introduction

Idiopathic pulmonary arterial hypertension (IPAH) is a life-threatening disease characterized by a marked and sustained elevation of pulmonary artery pressure. The disease results in RV failure and death (1). Current therapeutic approaches for the treatment of chronic pulmonary hypertension mainly provide symptomatic relief, as well as some improvement of prognosis. Although postulated for all treatments, evidence for direct antiproliferative effects of most approaches is missing (2–4). In addition, the use of most of the currently applied agents is hampered by either undesired side effects or inconvenient drug administration routes. Pathological changes in hypertensive pulmonary arteries include endothelial injury, proliferation, and hypercontraction of vascular SMCs (5).

Several growth factors have been implicated in the abnormal proliferation and migration of SMCs, including PDGF, basic FGF (bFGF), and EGF (6–10). In vitro studies established that PDGF acts as a potent mitogen and chemoattractant for SMCs (10). Active PDGF is built up by polypeptides (A and B chain) that form homo- or heterodimers and stimulate α and β cell surface receptors (11). Recently, 2 additional PDGF genes were identified, encoding PDGF-C and PDGF-D polypeptides (12–14). The PDGF receptors (PDGFRs) belong to a family of transmembrane receptor tyrosine kinases (RTKs) and are supposed to be held together by the bivalent PDGF ligands. This complex of dimeric receptor and PDGF results in an autophosphorylation of the RTK and an increase in kinase activity.

Both receptors activate the major signaling transduction pathways, including Ras/MAPK, PI3K, and phospholipase Cγ (11, 15, 16). Recently, upregulation of both PDGFRα and PDGFRβ has been shown in lambs with chronic intrauterine pulmonary hypertension (9). Pulmonary PDGF-A or PDGF-B mRNA, however, did not differ between pulmonary hypertensive and control animals. In lung biopsies from patients with severe pulmonary arterial hypertension (PAH), PDGF-A chain expression was significantly increased (17).

STI571 (imatinib or Gleevec) was designed to target the ATP-binding site of tyrosine kinases and is a well-established inhibitor of the kinase BCR-ABL; the receptor for the stem cell factor, c-KIT; and the PDGFR with IC_{50} values in the range of 0.1 μM (18). Currently, this substance is approved for the treatment of chronic myelogenous leukemia (CML) (19) and progressed malignant gastrointestinal stromal tumors (20). According to our current hypothesis, altered PDGF signaling might also play an important role in the course of PAH. Thus, we investigated the effects of STI571 on hemodynamics and pulmonary vascular remodeling in an established model of experimental pulmonary hypertension. In addition, downstream effects on the cellular and molecular level were analyzed to provide mechanistic explanation of STI571-induced changes.

Results

Effects of STI571 on hemodynamics and gas exchange. The rats challenged with monocrotaline (MCT) developed severe pulmonary hypertension within 28 days, which was sustained (if the animals survived) until day 42. Consequently, RV systolic pressure (RVSP) was increased significantly as compared with the saline-challenged group (Figure 1A). STI571 was applied by daily i.p. injections from day 28 to 42 and reversed chronic pulmonary hypertension to near-normal levels in the 50 mg/kg/d group (Figure 1, A and B). Telemetric measurement of RVSP showed that severe pulmonary
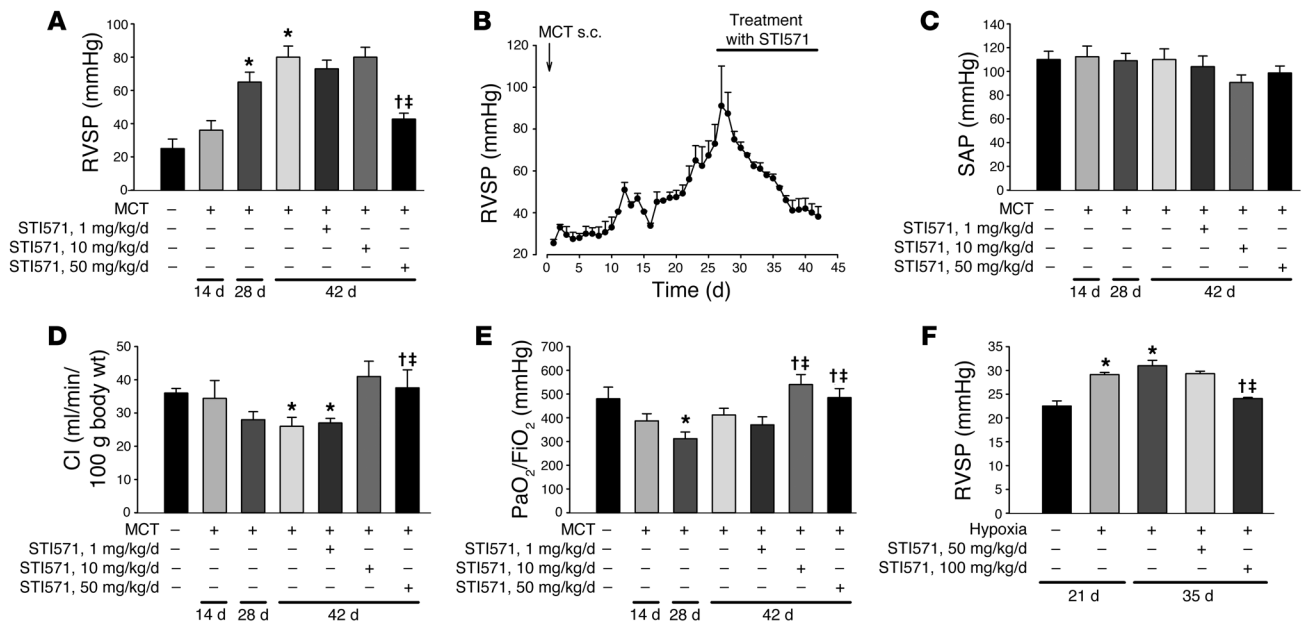
Figure 1
Impact of STI571 treatment on hemodynamics and gas exchange in MCT- and hypoxia-induced pulmonary hypertension. (**A**) RVSP (in mmHg) in the different treatment groups is shown. (**B**) Effect of STI571 on the course of RVSP in MCT-induced pulmonary hypertension measured by telemetry. MCT (s.c.) was applied at day 0 after animals had recovered from surgery for catheter implantation. Pulmonary hypertension developed progressively until day 28. STI571 was applied by daily i.p. injections at a dose of 50 mg/kg/d from day 28 to 42. In addition, systemic arterial pressure (SAP; in mmHg) (**C**), cardiac index (CI; in ml/min per 100 g body weight) (**D**), and oxygenation index (PaO$_2$/FiO$_2$) (**E**) are given for the different experimental groups. STI571 was applied at doses of 1, 10, and 50 mg/kg/d. (**F**) RVSP (in mmHg) in the different treatment groups of chronically hypoxic mice. STI571 was applied at doses of 50 and 100 mg/kg/d by gavage from day 21 to 35. *$P < 0.05$ versus control; †$P < 0.05$ versus MCT at day 28 or hypoxia at day 21; ‡$P < 0.05$ versus MCT at day 42 or hypoxia at day 35.

hypertension was established after 28 days and that STI571 nearly normalized pulmonary pressure at a dose of 50 mg/kg/d (Figure 1B). Mean systemic arterial pressure did not change in any of the treatment groups (Figure 1C). As compared with control animals (36.0 ± 1.4 ml/min per 100 g body weight), cardiac index was decreased in the MCT group at days 28 (28.0 ± 2.4 ml/min per 100 g body weight) and 42 (26.0 ± 2.7 ml/min 100 g per body weight; $P < 0.05$). In the STI571-treated animals (50 mg/kg/d), cardiac index increased significantly as compared with sham treatment (37.6 ± 5.4 ml/min 100 g body weight; $P < 0.05$) (Figure 1D). Similar results

were observed for arterial oxygenation, which decreased in MCT-challenged animals and significantly increased under treatment with STI571 at the doses of 10 and 50 mg/kg/d (Figure 1E).

In chronically hypoxic mice, severe pulmonary hypertension developed within 21 days, which was characterized by a significant increase in RVSP as compared with normoxic animals (Figure 1F). RVSP increased further until day 35 and was nearly normalized in the 100 mg ST571/kg/d group.

Effects of STI571 on right heart hypertrophy and animal survival. In the MCT groups, a significant RV hypertrophy developed as a conse-
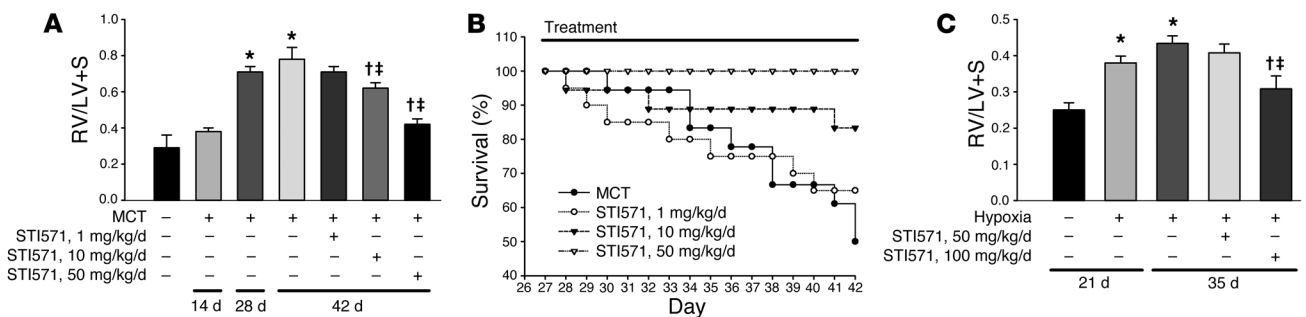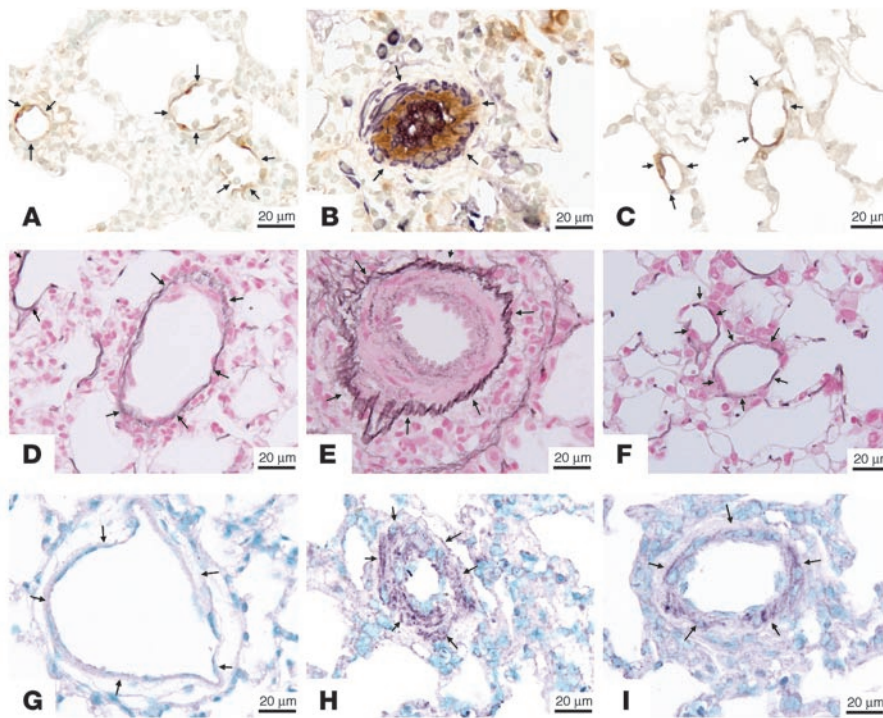

Figure 2
Effects of STI571 on right heart hypertrophy and survival. Ratio of RV to LV plus septum weight (RV/LV+S) (**A**) and survival rates of STI571-treated versus sham-treated (MCT control; filled circles) animals (**B**) are shown. Treatment at doses of 1, 10, and 50 mg/kg/d was started at day 28 after MCT injection; the different doses are indicated. (**C**) RV/LV+S values of chronically hypoxic mice. STI571 was applied at doses of 50 and 100 mg/kg/d by gavage from day 21–35. *$P < 0.05$ versus control; †$P < 0.05$ versus MCT at day 28 or hypoxia at day 21; ‡$P < 0.05$ versus MCT at day 42 or hypoxia at day 35.

Figure 3
Effects of STI571 on the degree of muscularization (**A**–**C**), medial wall thickness of small pulmonary arteries (**D**–**F**), and PDGF-B expression (**G**–**I**). **A**, **D**, and **G**: Day 0. **B**, **E**, and **H**: Day 42. **C**, **F**, and **I**: Day 42 treated with 50 mg/kg/d STI571. (**A**–**C**) The degree of muscularization is demonstrated by von Willebrand (brown) and α–smooth muscle actin (purple) staining for identifying endothelium and vascular SMCs, respectively. (**D**–**F**) Changes in medial wall thickness in pulmonary arteries are demonstrated. (**G**–**I**) PDGF-B staining is demonstrated in the medial layer of small pulmonary arteries. Scale bars: 20 μm. The arrows indicate pulmonary arteries.

quence of increased pulmonary pressures. The ratio of RV weight to LV plus septum weight (RV/LV+S) increased from 0.30 ± 0.02 (controls) to 0.71 ± 0.03 (28 days after MCT challenge) and 0.78 ± 0.07 (42 days after MCT challenge) (both $P < 0.05$ versus controls). STI571 caused a dose-dependent reduction of this ratio to 0.71 ± 0.03 (1 mg/kg/d), 0.62 ± 0.03 (10 mg/kg/d; $P < 0.05$ versus MCT), and 0.42 ± 0.03 (50 mg/kg/d; $P < 0.05$ versus MCT) (Figure 2A).

In the untreated MCT group, survival rate at day 42 was reduced to 50% (10 of 20 animals survived) (Figure 2B). STI571 treatment improved the survival rate to 65% (13 of 20) in the 1 mg/kg day group, 83.3% (15 of 18) in the 10 mg/kg/d group, and 100% (18 of 18) in the 50 mg/kg/d group.

The RV/LV+S ratio in hypoxic mice increased from 0.25 ± 0.02 (controls) to 0.38 ± 0.02 (21-day hypoxia) and 0.43 ± 0.02 (35-day hypoxia) (both $P < 0.05$ versus controls) (Figure 2C). In the 100 mg/kg/d treatment group, this ratio was decreased to 0.30 ± 0.03 ($P < 0.01$ versus hypoxia).

Antiremodeling potency of STI571 in pulmonary vasculature. We quantitatively assessed the degree of muscularization of pulmonary arteries with a diameter between 25 and 50 μm. In controls, the majority of vessels of this diameter were usually nonmuscularized, as shown exemplarily in Figure 3A. In the MCT-injected animals, both at day 28 and day 42, a dramatic decrease in nonmuscularized pulmonary arteries occurred (Figure 4A) with a concomitant increase in fully muscularized pulmonary arteries (Figures 3B and 4A). Treatment with STI571 at 50 mg/kg/d resulted in a significant reduction in fully muscularized arteries as compared with both MCT groups and increased the percentage of nonmuscularized pulmonary arteries (Figures 3C and 4A). Medial wall thickness of pulmonary arteries 25–50 μm in diameter was markedly increased in the MCT groups, both at day 28 (28.74% ± 0.33%; $P < 0.05$ versus control) and day 42 (36.83% ± 0.54%; $P < 0.05$ versus control), as compared with control animals (18.59% ± 0.42%) (Figure 3, D–F,

and Figure 4B). Compared with both MCT groups, STI571 at 50 mg/kg/d significantly reversed the increase in medial wall thickness to 22.66% ± 0.23% ($P < 0.05$ versus MCT).

Medial wall thickness of pulmonary arteries sized between 51 and 100 μm and more than 100 μm in diameter was determined separately. In both categories, STI571 nearly normalized medial wall thickness values (Figure 4, C and D). Lumen area (given in micrometers^2) of pulmonary arteries 25–50 μm in diameter decreased from 1,220 μm^2 to 1,075 μm^2 in the MCT 28-day group and to 791 μm^2 in the MCT 42-day group (Figure 4E). Treatment with STI571 at 50 mg/kg/d resulted in a normalization of internal lumen area (1,195 μm^2; $P < 0.05$ versus MCT).

In hypoxic animals, both at day 21 and day 35, a significant decrease in nonmuscularized pulmonary arteries occurred, with a concomitant increase in fully muscularized pulmonary arteries (Figure 4F). Treatment with 100 mg/kg/d STI571 resulted in a significant reduction in partially muscularized arteries as compared with both hypoxia groups (21 days, i.e., before the start of STI571 treatment, and 35 days) and increased significantly the percentage of nonmuscularized pulmonary arteries.

Effects of STI571 on MMP activity. The levels of MMP-2 and MMP-9 protein were markedly increased in lung homogenates of MCT-challenged rats when compared with controls. This increase was normalized by STI571 treatment (Figure 5A). Zymographic measurement of MMP revealed highly elevated activity in MCT-challenged animals, with most prominent effects observed for MMP-2 (Figure 5B). Protein content of MMP-2 as well as activity were normalized in the STI571-treated animals (50 mg/kg/d).

Effects of STI571 on PDGF-B and PDGFR expression and phosphorylation. In MCT-treated animals, a marked increase in PDGF-B protein was detected (by immunohistochemistry) in the medial layer of small pulmonary arteries, while control lungs were completely negative (Figure 3, G and H). As compared with MCT-challenged
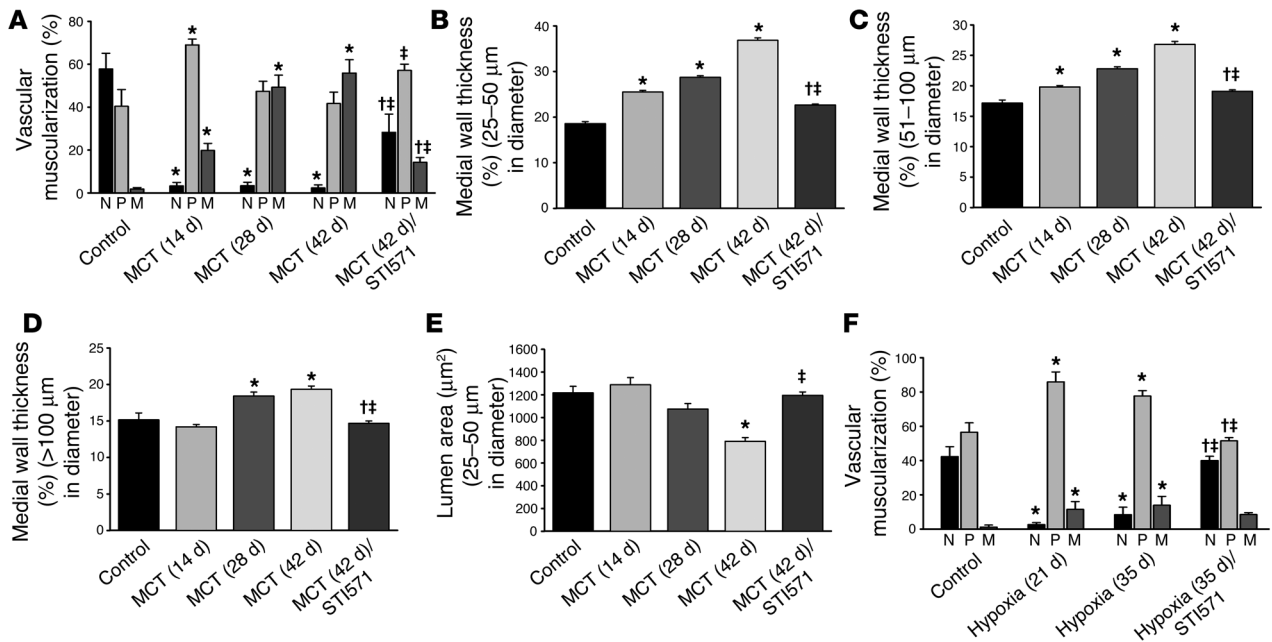
Figure 4

Effects of STI571 on the degree of muscularization; medial wall thickness of pulmonary arteries sized 25–50 μm, 51–100 μm, and greater than 100 μm; and internal lumen area of pulmonary arteries sized 25–50 μm. (**A**) Proportion of non- (N), partially (P), or fully (M) muscularized pulmonary arteries, as percentage of total pulmonary artery cross section (sized 25–50 μm). A total of 60–80 intraacinar vessels was analyzed in each lung. (**B**–**D**) Medial wall thickness of pulmonary arteries sized 25–50 μm (**B**); 51–100 μm (**C**); and greater than 100 μm (**D**). (**E**) The internal lumen area of vessels between 25 and 50 μm. Results from rats exposed to MCT for 28 and 42 days and STI571-treated rats (treatment from day 28 to 42 with 50 mg/kg/d) are presented. (**F**) Proportion of non-, partially, or fully muscularized pulmonary arteries from chronically hypoxic mice treated with STI571 (sized 20–70 μm). STI571 was applied at a dose of 100 mg/kg/d by gavage from day 21 to 35. *$P < 0.05$ versus control; [†]$P < 0.05$ versus MCT at day 28 or hypoxia at day 21; [‡]$P < 0.05$ versus MCT at day 42 or hypoxia at day 35.

rats, the STI571-treated animals displayed lower PDGF-B expression in the pulmonary vasculature (Figure 3I). PDGFRβ protein and its phosphorylated (activated) form were highly upregulated in MCT-challenged rats (Figure 6) and mice (Figure 7). Similar results were obtained for the ERK1/2 phosphorylation in rats (Figure 8). In contrast, expression and phosphorylation of both PDGFR and ERK1/2 were strongly suppressed by treatment with 50 mg/kg/d STI571 in rats (Figures 6 and 8), and phosphorylation of the PDGFR was reduced in hypoxic mice treated with 100 mg/kg/d STI571 (Figure 7).

Expression of PDGFRβ in lungs from patients with PAH. Western blot analysis revealed a significant increase in protein expression of PDGFRβ and its phosphorylated (activated) form in IPAH lungs compared with healthy donor lungs (Figure 9).

STI571 inhibits pulmonary SMC proliferation in vitro. Rat pulmonary artery SMC (PA-SMC) proliferation, induced by 10% FBS/DMEM, was inhibited by STI571 in a dose-dependent manner (0.1, 1, and 5 μM), as determined by [³H]thymidine incorporation assay (Figure 10A). In addition, STI571 increased the apoptosis of PA-SMCs in

the presence of 10% serum in a dose-dependent manner (Figure 10B). In order to determine the selectivity of STI571 on PDGF-induced SMC proliferation, different growth factors (PDGF-AA, PDGF-BB, IGF-1, EGF, or bFGF) were employed to stimulate rat
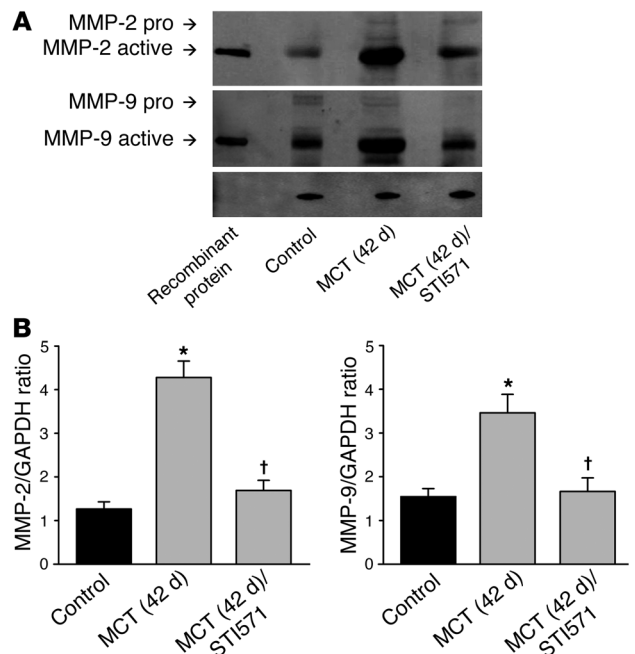

Figure 5

MMP expression (**A**) and densitometric quantification (**B**) in pulmonary arteries. Homogenates of lung tissue were examined from MCT-challenged animals receiving STI571 at 50 mg/kg/d, as compared with controls and nontreated MCT animals. Western blots for the pro and active forms of MMP-2 and MMP-9 (**A**) and densitometric quantification normalized to GAPDH (**B**) are shown. *$P < 0.05$ versus control; [†]$P < 0.05$ versus MCT at day 42.
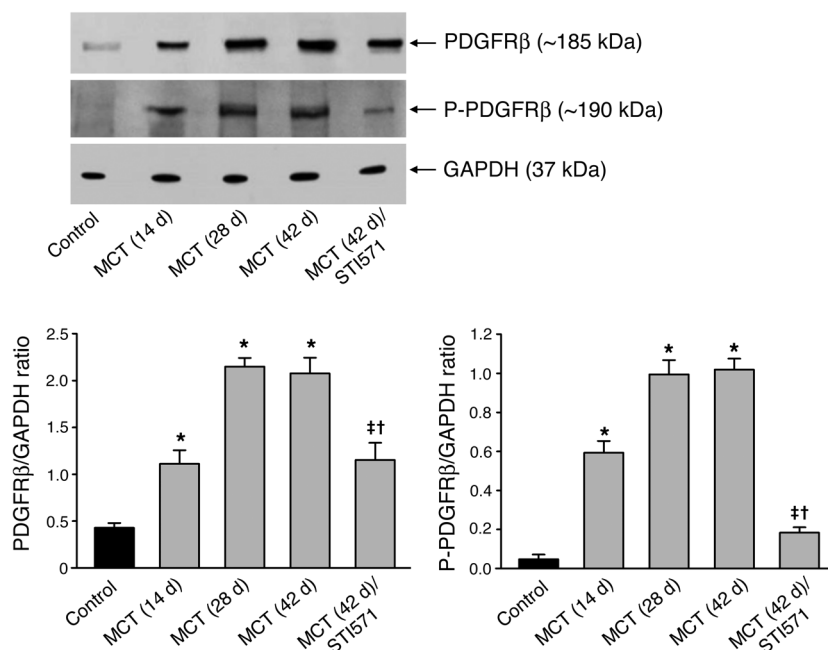
Figure 6
Increased PDGFRβ expression/phosphorylation in MCT-induced pulmonary hypertension. Western blot analysis was used to assess expression of PDGFRβ and PDGFRβ phosphorylation (P-PDGFRβ) in rat lungs from controls and animals treated with MCT (14 days), MCT (28 days), MCT (42 days), and MCT (42 days)/STI571. Immunoblots are representative of 4 individual lungs from each group, showing identical results. Quantification of PDGFRβ and PDGFRβ phosphorylation is shown in the bar graphs. PDGFRβ and PDGFRβ phosphorylation are normalized to GAPDH. *$P < 0.05$ versus control; †$P < 0.05$ versus MCT at day 28; ‡$P < 0.05$ versus MCT at day 42.

pulmonary SMCs. STI571 was added to the culture medium at 1 μM 2 hours before the addition of each growth factor. STI571 demonstrated a significant inhibition of PDGF-AA– and PDGF-BB–induced proliferation, while, in contrast, proliferation stimulated by IGF-1, EGF, or bFGF was unaffected (Figure 10C).

Effect of STI571 on PA-SMC proliferation and apoptosis. In MCT-challenged rats, proliferating cell nuclear antigen (PCNA) labeling showed proliferation of SMCs in distal pulmonary arteries as compared with controls (Figure 11A). In parallel to normalization of vessel morphology, the number of PCNA-positive cells was considerably reduced in animals treated with STI571. Virtually no apoptosis was detected by TUNEL assay in pulmonary resistance vessels of control and MCT-challenged animals. However, the number of cells undergoing apoptosis was considerably increased in pulmonary arterial vessel walls in the STI571 group (Figure 11B).

Discussion

The novel finding of the present study is that the PDGFR antagonist STI571 is an effective treatment in 2 well-established experimental models of severe pulmonary hypertension. Treatment effects showed dose dependency and included (a) reversal of pulmonary hypertension, (b) reduction in right heart hypertrophy and improvement in cardiac output, (c) reversal of pulmonary vessel proliferation, and (d) an impressive survival benefit in

Figure 7
Increased PDGFRβ expression/phosphorylation in hypoxia-induced pulmonary hypertension. Western blot analysis was used to assess expression of PDGFRβ and PDGFRβ phosphorylation in mouse lungs from controls and animals treated with hypoxia (35 days) and hypoxia (35 days)/STI571. Immunoblots are representative of 4 individual lungs from each group, showing identical results. Quantification of PDGFRβ and PDGFRβ phosphorylation is shown in the bar graphs. PDGFRβ and PDGFRβ phosphorylation are normalized to GAPDH. *$P < 0.05$ versus control; †$P < 0.05$ versus MCT at day 28.
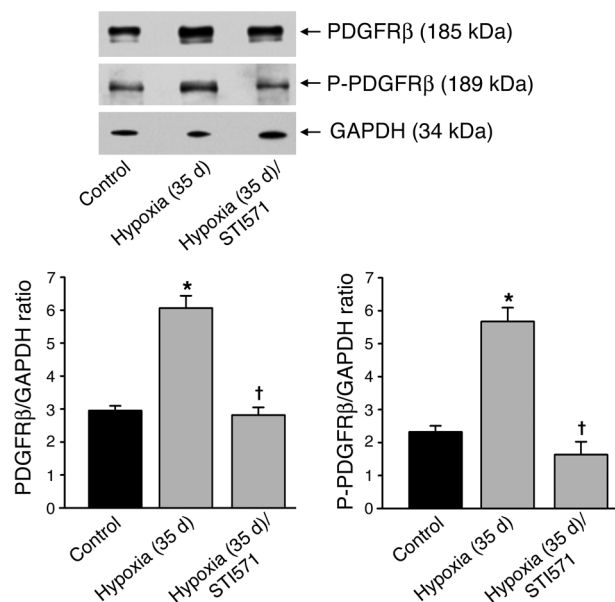
MCT rats. Moreover, the importance of PDGF signaling in the course of pulmonary hypertension was proven by a significant inhibition of PDGF-associated signaling pathways by STI571.

Recently, new therapeutic approaches have been proposed for the treatment of chronic pulmonary hypertension in affected patients. These include endothelin receptor antagonists (4), nonparenteral prostanoids (21), and phosphodiesterase 5 inhibitors (22–25). However, all of these approaches address pulmonary vasodilation as the main therapeutic target; although postulated, there is little proof (either experimental or clinical) that any of these drugs has a direct antiproliferative effect or even the potency to reverse proliferative changes in the pulmonary circulation.

PDGFR signaling–related cellular proliferation has been suggested as an important contributor to the development and progres-
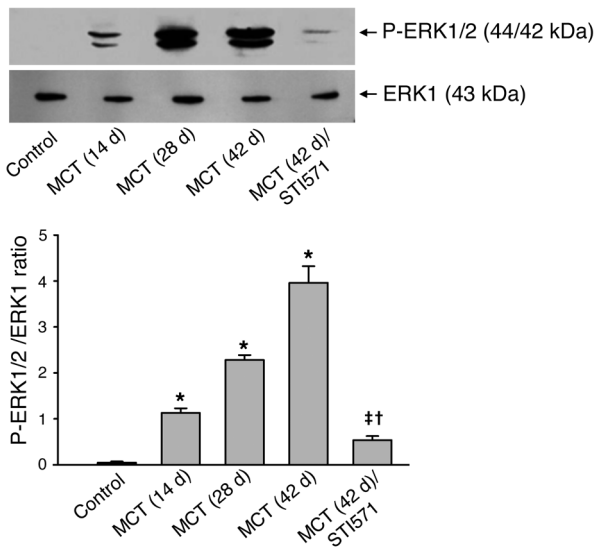
Figure 8
Increased PDGFRβ signaling (ERK1/2 phosphorylation) in MCT-induced pulmonary hypertension. Western blot analysis was used to assess expression of ERK1/2 phosphorylation (P-ERK1/2) in rat lungs from controls and animals treated with MCT (14 days), MCT (28 days), MCT (42 days), and MCT (42 days)/STI571. Immunoblots are representative of 4 individual lungs from each group, showing identical results. Quantification of ERK1/2 phosphorylation is shown in the bar graph. ERK1/2 phosphorylation is normalized to ERK1. *$P < 0.05$ versus control; †$P < 0.05$ versus MCT at day 28; ‡$P < 0.05$ versus MCT at day 42.

sion of pulmonary hypertension (9, 17, 26, 27). A recently published study investigated the effects of a truncated soluble PDGFRβ in the development of hyperoxia-induced vascular changes and found reduced SMC proliferation (28). In addition, Balasubramaniam et al. prevented the development of pulmonary hypertension in the ovine fetus employing an aptamer that selectively inhibits PDGF-B (9). However, up to now, no interventional data have been available describing the therapeutic use of the specific PDGFR antagonist STI571 in experimental or clinical pulmonary hypertension. In our current study, we found a most prominent reversal of pulmonary hypertension in response to STI571 therapy. Treatment did not affect systemic arterial pressure, proving selectivity of this approach for the abnormal pulmonary circulation and providing evidence for the absence of noteworthy vasodilatory effects. In patients suffering from severe pulmonary hypertension, inadequate adaptation of cardiac output represents the main limitation for normal physical activities. In addition, an insufficient increase in systemic arterial pressure under conditions of exercise is a negative predictor of survival for patients with severe PAH (29). In advanced stages of right heart load, systemic arterial pressure is already reduced at rest. Thus, agents affecting systemic blood pressure, such as nonselective vasodilators — though lowering pulmonary pressures to a certain extent — provoke undesirable systemic hypotension. In view of this clinically relevant aspect, antiproliferative agents such as STI571, which completely lack acute vasodilative potential, represent what we believe to be an entirely novel approach for the treatment of chronic vascular diseases.

As a consequence of reduced right heart load, muscular cardiac hypertrophy was reverted to near normal levels in a dose-depend-

ent manner in both MCT-treated rats and chronically hypoxic mice. Taken together with the improved survival, these data are strongly suggestive for a curative potential of PDGFR inhibition in severe pulmonary hypertension regardless of the initiating event. Although treatment efficacy has also been shown to a certain extent for serine elastase inhibitors (30), simvastatin (31), fasudil (a Rho-kinase inhibitor) (32), or phosphodiesterase inhibitors (33, 34), the overall treatment efficacy (including hemodynamics, right heart hypertrophy, vascular remodeling, and survival, as currently presented) has not been shown before.

Upon treatment with STI571, the proportion of non- to fully muscularized vessels dramatically increased in MCT- and hypoxia-induced pulmonary hypertension. Structural changes observed in MCT-induced pulmonary hypertension strongly resemble characteristics of human PAH in terms of (a) marked medial wall thickening, (b) intimal proliferation, and (c) plexiform lesion formation, all resulting in a dramatic loss of resistance vessel capacity (35). As a consequence, hemodynamics and remodeling of the right heart in chronically affected animals at late stages of the disease mimic well the situation found in patients (36, 37). In addition, hypoxia is the main stimulus for the induction of pulmonary hypertension accompanying chronic ventilatory disorders such as chronic obstructive pulmonary disease and interstitial lung disease. While acute hypoxia causes selective pulmonary arteriolar vasoconstriction, chronic exposure to hypoxia results in morphological and functional changes in the pulmonary vascular bed (24, 25, 38, 39). Hypoxia may also be an activator of the PDGF-related pathway, as previously shown in HT1080 cells (40).

In the current study, we found a marked increase in cell proliferation (assessed by PCNA staining) in pulmonary resistance vessels of MCT-challenged animals. Interestingly, considerable apoptosis was found neither in control animals nor in those with MCT-induced pulmonary hypertension. However, STI571 treatment resulted in near normal vessel morphology, reduced proliferation rate, and,
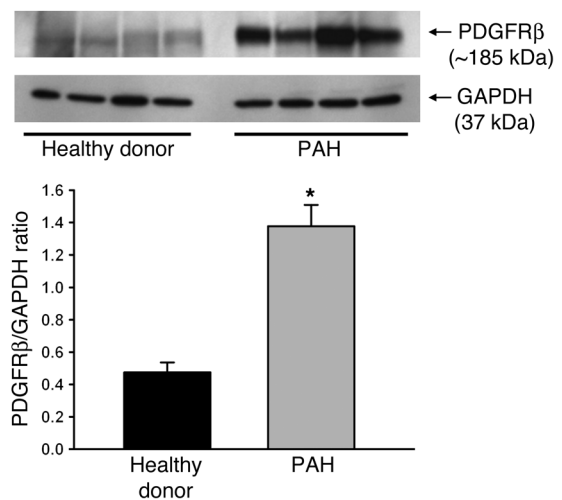

Figure 9
Change in expression of PDGFRβ in PAH lungs. Expression of PDGFRβ in lung homogenates from patients with PAH ($n = 4$) and healthy donors ($n = 4$) and densitometric quantification of the signal intensity. Western blot analysis was performed with anti-PDGFRβ antibody. The specific antibody recognizes protein at a molecular weight of ~185 kDa. Quantification of PDGFRβ is shown in the bar graph. *$P < 0.05$ versus control.
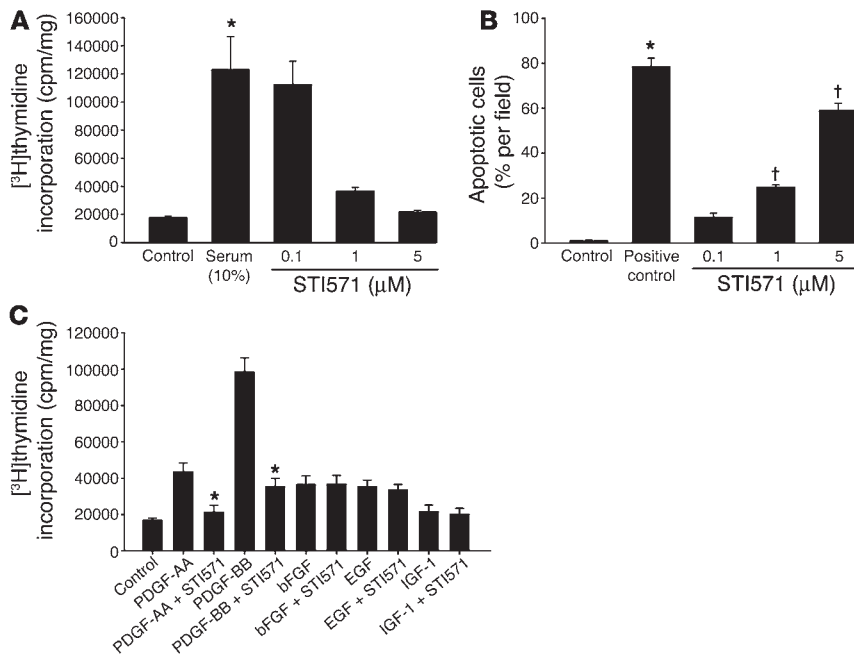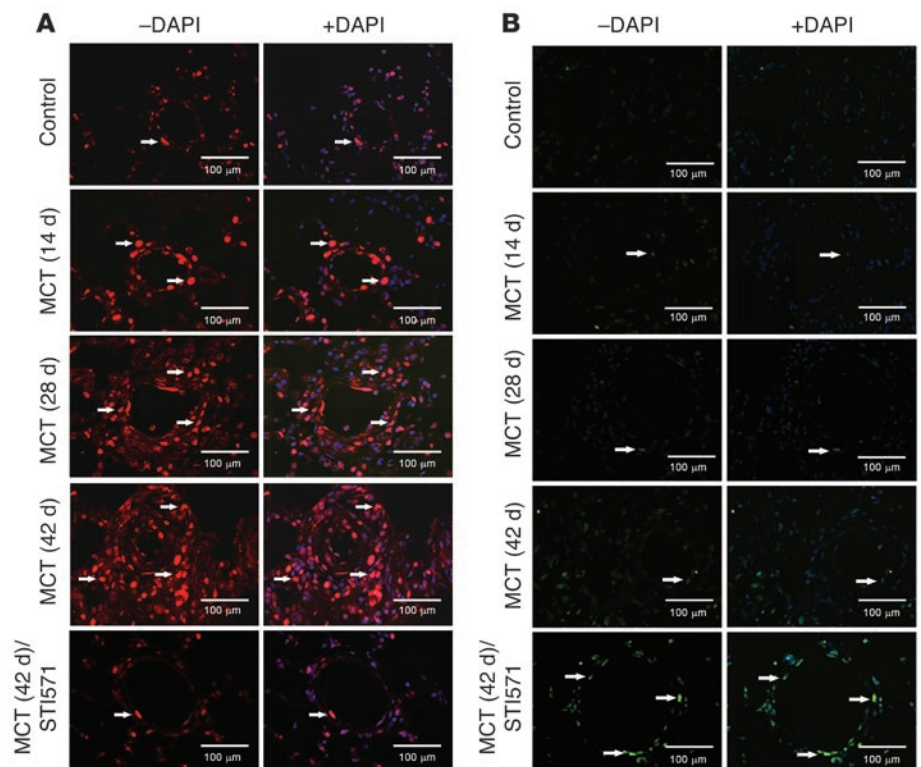
Figure 10
Effect of STI571 on serum-induced proliferation ([³H]thymidine incorporation) (**A**), apoptosis (**B**) and PDGF-AA–, PDGF-BB–, IGF-1–, EGF-, or bFGF-induced proliferation (**C**) in pulmonary rat SMCs. STI571 dose-dependently inhibited proliferation of pulmonary artery rat SMCs stimulated with 10% FBS/DMEM. For comparison, values for control cells maintained in 0.1% FBS are given. Values are expressed as counts per minute/milligram protein or percent per field derived from 6–8 separate isolates. *P < 0.05 versus control; †P < 0.05 versus serum (10%) or the different growth factors.

most interestingly, an increased apoptosis rate in the vessel wall. This is well in line with previous findings in which antiproliferative properties of STI571 were attributed to an increased apoptosis rate in balloon-injured vessels of hypercholesterolemic rabbits (41). In this context, PDGF is known to be a potent inhibitor of apoptosis, thereby promoting proliferation in several tissues (42, 43) predominantly via the PI3K/Akt pathway (44, 45). Thus, inhibition of proliferation by STI571 can in part be explained by suppression of

the antiapoptotic properties of PDGF signaling. Moreover, recent reports indicate both c-ABL–dependent and –independent induction of apoptosis by STI571 via the activation of caspases (46, 47).

Increase in MMP expression and activity has been shown to correlate with the severity of disease in various experimental forms of pulmonary hypertension (33, 34, 38). MMP-9 is strongly induced by ERK activities, which are known to be involved in downstream signaling of PDGFR activation (48). Furthermore, in vitro stud-

Figure 11
Effect of STI571 on rat PA-SMC proliferation (**A**) and apoptosis (**B**) in MCT-induced pulmonary hypertension. Medial hypertrophy of pulmonary resistance vessels was associated with an increased number of proliferating vascular cells in MCT-induced pulmonary hypertension. Immunohistochemistry for PCNA (red nuclei are PCNA-positive cells; **A**) revealed increased proliferation in MCT-challenged animals (as compared with controls). Regression of medial hypertrophy induced by STI571 (50 mg/kg/d) was attributed to reduced SMC proliferation. Apoptosis (assessed by in situ TUNEL assay) was virtually absent in control animals and very low in pulmonary arteries from MCT animals at different time points. Apoptosis (green cells are TUNEL-positive cells; **B**) was increased in animals treated with STI571. Scale bar: 100 μm. Arrows indicate PCNA- and TUNEL- positive cells in **A** and **B**, respectively.
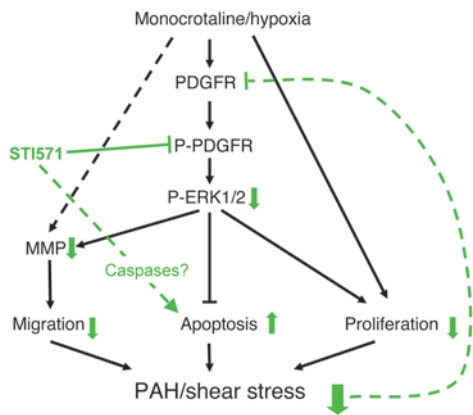
Figure 12
Schematic illustration of the proposed signaling events in MCT- or hypoxia-induced pulmonary hypertension and the impact of STI571. This scheme depicts the proposed mechanism of disease induction by MCT or hypoxia and the possible interaction of STI571 with the involved signaling events. Induction of pathways and/or cellular events is symbolized by black arrows (solid lines indicate proven evidence; dashed lines indicate postulated mechanisms). Green lines and arrows indicate the actions of STI571 in this model.

ies provided evidence for direct MMP-1 and MMP-3 induction by PDGF-A (49) and PDGF-B (50), respectively. Moreover, reduction in MMP-2 levels parallels hemodynamic and structural changes upon onset of effective therapy (34). The present finding that STI571 strongly reduced MMP-2 and MMP-9 expression and activity is thus well in line with the beneficial effect of this agent on MCT-induced structural and hemodynamic changes.

Direct evidence for an involvement of the PDGFR signaling pathway in the development of MCT-induced pulmonary hypertension and in the therapeutic effects of STI571 was derived from the following findings: (a) PDGFRβ expression was strongly upregulated in the MCT-challenged rat lungs — this is well in line with previous data that have shown that PDGFRβ mRNA was significantly increased in the pulmonary artery of MCT-treated rats (9, 27); (b) this increased expression was reversed with STI571 treatment, in parallel to the beneficial effects on hemodynamics, morphology, and survival; (c) PDGFRβ phosphorylation was increased in MCT-challenged animals but reduced in response to STI571 treatment; and (d) induction of downstream signaling of the PDGFR pathway was indicated by activation (MCT alone) and suppression (MCT plus STI571) of ERK1/2. ERK phosphorylation has been shown to be a key downstream signal for PDGFR stimulation (51, 52), and its strong suppression under STI571 supports the notion that this agent is operative via the PDGFR system (Figure 12). It is well known that, besides the PDGFR, STI571 is also blocking ABL tyrosine kinases and c-kit with identical IC_{50} values of 100 nM. BCL-ABL transformation is specifically described for CML and does not play a role in nonmalignant pulmonary diseases. Little is known about the role of c-kit–positive bone marrow–derived hematopoietic stem cells in pulmonary diseases. If at all, a single report exists that shows some beneficial potential of these cells in a lung injury model (53). Thus, interaction with this pathway is highly unlikely to be involved in the currently described study. Therefore, the PDGF-inhibitory capacity of STI571 is most likely the predominant mode of action involved in the beneficial therapeutic effects in both

PAH models. Further evidence for the selectivity of STI571 for the PDGFR was obtained from cell culture experiments in which different growth factors (PDGF-AA, PDGF-BB, IGF-1, EGF, and bFGF) were employed to stimulate pulmonary arterial SMC growth. Similar results have previously been shown for proliferating rat coronary SMCs demonstrating that an investigational PDGFR antagonist that is clinically not applicable (CGP 57148B) selectively blocked PDGF-AA– or PDGF-BB–induced proliferation (54).

Furthermore, we believe that PDGFR upregulation and activation of the consecutive signaling pathway (PDGFR phosphorylation/ERK) represent a self-perpetuating vicious circle, which, regardless of the primary inducer (MCT or hypoxia), via loss of vessel potency and increased shear stress results in further pulmonary vascular remodeling. It is well known that shear stress is a strong stimulus for PDGF and PDGFR expression in vascular cells (27, 55, 56). Once downstream signaling of the PDGFR is inhibited by STI571 and thereby vascular remodeling is reversed (as shown in our experiments), this vicious circle is interrupted, and PDGFR is consecutively downregulated.

Our study is the first to our knowledge to describe the successful therapeutic use of the PDGFR inhibitor STI571 in 2 well-accepted animal models of pulmonary hypertension. We demonstrate that treatment with STI571 not only reversed hemodynamic and structural changes provoked by MCT but also impressively improved survival of the rats in the MCT rat model. Furthermore, evidence for the involvement of the PDGFR system in disease development and response to therapy was provided on the cellular and molecular level. Taking into account the limitations of experimental studies, we still believe that our findings will be stimulating for consideration of this novel therapeutic approach in patients suffering from life-threatening advanced pulmonary hypertension, in which PDGFRβ may be strongly upregulated, as suggested by the findings in the currently investigated PAH patients. As STI571 is already broadly used as an anti-cancer drug and proved to be well tolerated in these indications, the clinical development as a new therapy for pulmonary hypertension might therefore be imminent.

Methods

Experimental design. Adult male Sprague-Dawley rats (300–350 g in body weight; Charles River Laboratories) were randomized for treatment 28 days after a s.c. injection of saline or 60 mg/kg MCT (Sigma-Aldrich) to induce pulmonary hypertension. In addition to a group of untreated rats, the experimental groups included rats that received once-daily i.p. injection of STI571 (imatinib; gift from S. Pascoe and E. Buchdunger, Novartis, Novartis Horsham Research Centre, Horsham, United Kingdom) at a dose of 50 mg/kg or the administration vehicle (isotonic saline). Rats were examined after 14 days of treatment (on day 42). STI571 is a low-molecular-weight inhibitor of the protein tyrosine kinase activity of both PDGFR subtypes (57, 58). STI571 was chosen to target the PDGF signaling in MCT-induced vascular disease, and the dose was calculated based on published studies (59).

Hypoxic pulmonary vascular remodeling was induced by exposure of mice (8-week-old C57BL/6) to chronic hypoxia (10% O_2) in a ventilated chamber, as described previously (39). The chronic effects of STI571 were assessed in mice exposed to hypoxia for 35 days. Briefly, 20 animals were kept in hypoxic conditions to develop pulmonary hypertension. After 21 days, animals were randomized to receive either oral STI571 (50 and 100 mg/kg/d) or placebo via gavage.

All protocols were approved by the Animal Care Committee of the University Giessen.

Surgical preparation and tissue preparation. For monitoring hemodynamics, the animals were initially anesthetized i.p. with ketamine and xylazine. The left carotid artery was cannulated, and a right heart catheter was inserted through the right jugular vein for measurement of RV pressure with fluid-filled force transducers. Cardiac output in rats was measured by thermodilution technique (Cardiotherm 500-X; Hugo-Sachs Electronic — Harvard Apparatus GmbH) as described previously (33, 34). After exsanguination, the left lung was fixed for histology in 10% neutral buffered formalin, and the right lung was snap-frozen in liquid nitrogen.

Telemetric measurement of RV pressure. RV pressure in rats was measured with an implanted radiotelemetry system (Dataquest A.R.T. 2.1; Data Sciences Inc.). The transmitter (model TA11PA) is connected to a fluid-filled sensing catheter and transfers the signals to a remote receiver (model RPC-1) and a data-exchange matrix connected to a computer. Under anesthesia, the sensing catheter was inserted into the jugular vein and forwarded to the RV. The waveform was displayed on the computer and used to ensure correct positioning of the catheter. Animals were allowed to recover and were housed individually in standard rat cages. RV pressure was recorded at 1-hour intervals from the time of implantation.

Assessment of RV hypertrophy. The RV wall was separated from the LV wall and ventricular septum. Wet weight of the RV, free LV wall, and ventricular septum was determined. RV hypertrophy was expressed as the ratio of weight of the RV wall and that of the free LV wall and ventricular septum (LV+S).

Patient characteristics and measurements. Human lung tissue was obtained from 4 donors and 4 PAH patients (2 with IPAH, 1 with connective tissue disease–associated PAH, 1 with congenital heart disease) undergoing lung transplantation. Lung tissue was snap-frozen directly after explantation for mRNA and protein extraction. The study protocol for tissue donation was approved by the Ethk-Kommission am Fachbereich Humanmedizin der Justus-Liebig-Universitaet Giessen of the University Hospital Giessen (Giessen, Germany) in accordance with national law and with Good Clinical Practice/International Conference on Harmonisation guidelines. Written informed consent was obtained from each individual patient or the patient's next of kin.

Paraffin embedding and microscopy. Fixation was performed by immersion of the lungs in a 3% paraformaldehyde solution. For paraffin embedding, the entire lungs were dissected in tissue blocks from all lobes. Sectioning at 3 μm was performed from all paraffin-embedded blocks. H&E and elastica staining was performed according to common histopathological procedures. Analysis was done in a blinded fashion. To assess the type of remodeling of muscular pulmonary arteries, microscopic images were analyzed using a computerized morphometric system (QWin; Leica). In each rat, 60 to 80 intraacinar arteries were categorized as muscular (i.e., with a complete medial coat of muscle), partially muscular (i.e., with only a crescent of muscle), or nonmuscular (i.e., no apparent muscle), as previously reported (34). Lumen area was defined as the area within the lamina elastica interna, counted and averaged from 800 representative vessels within a range of diameters from 25 to 50 μm. Medial area is the area between the lamina elastica interna and the lamina elastica externa. Arteries were additionally categorized according to their external diameter. Category I included arteries with an external diameter between 20 and 50 μm; category II included arteries with an external diameter between 51 and 100 μm; and category III included arteries with an external diameter greater than 101 μm. In mouse sections, 60–80 intraacinar vessels at a size between 20 and 70 μm accompanying either alveolar ducts or alveoli were analyzed by an observer blinded to treatment in each mouse. As described above, each vessel was categorized as nonmuscularized, partially muscularized, or fully muscularized.

Gelatin zymography. Lung tissues were homogenized at 4°C in buffer containing 1% Triton X-100, 150 mM NaCl, 2.5 mM sodium pyrophosphate,

1 mM β-glycerophosphate, 10 μM E-64, and 20 mM Tris-HCl, pH 7.5, with 20 mg ml^{-1} ratio of tissue weight by buffer volume. Activity of MMPs was analyzed by SDS-PAGE zymography, in which the enzymes hydrolyze gelatin substrate present in the gel and form a clear band. Gels were visualized with a Biodoc analyzer (Biometra), where activity of MMP-2 and MMP-9 was shown as a clear white band against the blue background, as previously described (34).

Western blotting. Lung tissue samples were homogenized in lysis buffer containing 50 mM Tris-HCl, pH 7.4, 50 mM NaCl, 5 mM EDTA, 1% Triton X-100, 0.05% SDS, 50 mM NaF, 10 mM β-glycerophosphate, sodium pyrophosphate, 100 μM Na$_3$VO$_4$, and protease inhibitor cocktail (Roche Diagnostics Corp.). Lysates were normalized and separated on 7.5% or 10% polyacrylamide gels and transferred to PVDF membranes. After blocking, the membranes were probed with 1 of the following antibodies: anti-PDGFRβ (sc432), anti-phospho (Tyr1021)-PDGFRβ (sc12909-R), anti-ERK1/2 (sc93), and anti-phospho (Thr202/Tyr204/Thr185/Tyr 187)-ERK1/2 (sc16982-R) antibody (all from Santa Cruz Biotechnology Inc.), anti-MMP2, anti-MMP9, or anti-GAPDH loading control (all from Abcam Ltd.), followed by a 1 hour incubation with secondary antibodies conjugated with HRP. Bound antibodies were detected by chemiluminescence with the use of an ECL detection system (Amersham Biosciences) and quantified by densitometry.

Evaluation of in situ PA-SMC death and proliferation. To assess PA-SMC proliferation in rats treated with MCT alone or with STI571, PCNA was evaluated. Tissue sections were deparaffinized in xylene, then treated with a graded series of alcohol washes, rehydrated in PBS (pH 7.5), and incubated with antigen retrieval solution (Zymed Laboratories Inc.) in a water bath at 90°C for 20 minutes. Slides were then washed in PBS, incubated for 1 hour in a protein-blocking solution, and incubated overnight with anti-PCNA rabbit polyclonal antibody (Santa Cruz Biotechnology Inc.). Antibodies were washed off and incubated with Alexa 555–conjugated goat anti-rabbit IgG antibodies (Invitrogen Corp.). After incubation, all sections were counterstained with nuclear DAPI staining and mounted with Dako fluorescent mounting media (all from DakoCytomation).

To assess PA-SMC apoptosis, sections were visualized using the terminal deoxynucleotidyl transferase–mediated (TdT-mediated) TUNEL method with the help of In Situ Cell Death Detection Kit (Roche Diagnostics Corp.) as specified by the manufacturer. At the end of the procedure, the slides were observed by fluorescence microscopy after DAPI staining (DakoCytomation).

Proliferation assay. Primary rat SMCs were isolated, as previously described (60), and cultures were maintained at 37°C in a humidified 5% CO$_2$/95 % O$_2$ atmosphere. For assessment of proliferation, pulmonary rat SMCs from passage 2 were seeded in 12-well plates at a density of 4×10^4 cells/well in 10% FBS/DMEM. Cells were rendered quiescent by incubation in serum-free DMEM for 2 hours, followed by serum deprivation (DMEM containing 0.1% FBS) for 72 hours. Subsequently, they were stimulated with 10% FBS/DMEM to induce cell cycle reentry. After treatment with 0, 0.1, 1, and 5 μM STI571 during the last 12 hours and throughout the stimulation period, the cells were pulsed with 1.5 μCi per well [^{3}H]thymidine (Amersham Pharmacia Biotech Ltd.) during the last 12 hours of stimulation. The [^{3}H]thymidine content of cell lysates was determined by scintillation counting and normalized by protein concentration, which was measured by the Lowry method (61). To investigate the specificity of STI571 on PDGF-related proliferation, quiescent cells were stimulated with recombinant PDGF-AA or PDGF-BB (60 ng/ml in serum-free medium), IGF-1 (100 ng/ml), EGF (50 ng/ml), and bFGF (50 ng/ml). All growth factors were purchased from Upstate.

Apoptosis assay. The isolated PA-SMCs were grown on chamber slides and treated as indicated (0.1, 1, and 5 μM STI571). After 24 hours, cells were

fixed immediately in 4% (vol/vol) paraformaldehyde for 1 hour, permeabilized using Triton X-100 (Sigma-Aldrich), and then incubated at 37°C for 60 minutes with TdT-mediated TUNEL reaction mixture (In Situ Cell Death Detection Kit, Fluorescein; Roche Diagnostics Corp.). For positive control, cells were treated with DNase I (Roche Diagnostics Corp.) as specified by the manufacturer.

Data analysis. All data are given as mean ± SEM. Differences between groups were assessed by ANOVA and Student-Newman-Keuls post-hoc test for multiple comparisons, with a P value < 0.05 considered to be significant.

1. Humbert, M., Sitbon, O., and Simonneau, G. 2004. Treatment of pulmonary arterial hypertension. *N. Engl. J. Med.* **351**:1425–1436.
2. Barst, R.J., et al. 1996. A comparison of continuous intravenous epoprostenol (prostacyclin) with conventional therapy for primary pulmonary hypertension. The Primary Pulmonary Hypertension Study Group. *N. Engl. J. Med.* **334**:296–302.
3. Olschewski, H., et al. 2002. Inhaled iloprost for severe pulmonary hypertension. *N. Engl. J. Med.* **347**:322–329.
4. Rubin, L.J., et al. 2002. Bosentan therapy for pulmonary arterial hypertension. *N. Engl. J. Med.* **346**:896–903.
5. Humbert, M., et al. 2004. Cellular and molecular pathobiology of pulmonary arterial hypertension. *J. Am. Coll. Cardiol.* **43**:13S–24S.
6. Jones, P.L., Cowan, K.N., and Rabinovitch, M. 1997. Tenascin-C, proliferation and subendothelial fibronectin in progressive pulmonary vascular disease. *Am. J. Pathol.* **150**:1349–1360.
7. Ushio-Fukai, M., et al. 2001. Epidermal growth factor receptor transactivation by angiotensin II requires reactive oxygen species in vascular smooth muscle cells. *Arterioscler. Thromb. Vasc. Biol.* **21**:489–495.
8. Xin, X., Johnson, A.D., Scott-Burden, T., Engler, D., and Casscells, W. 1994. The predominant form of fibroblast growth factor receptor expressed by proliferating human arterial smooth muscle cells in culture is type I. *Biochem. Biophys. Res. Commun.* **204**:557–564.
9. Balasubramaniam, V., et al. 2003. Role of platelet-derived growth factor in vascular remodeling during pulmonary hypertension in the ovine fetus. *Am. J. Physiol. Lung Cell Mol. Physiol.* **284**:L826–L833.
10. Yu, Y., et al. 2003. PDGF stimulates pulmonary vascular smooth muscle cell proliferation by upregulating TRPC6 expression. *Am. J. Physiol. Cell Physiol.* **284**:C316–C330.
11. Heldin, C.H., and Westermark, B. 1999. Mechanism of action and in vivo role of platelet-derived growth factor. *Physiol. Rev.* **79**:1283–1316.
12. Bergsten, E., et al. 2001. PDGF-D is a specific, protease-activated ligand for the PDGF beta-receptor. *Nat. Cell Biol.* **3**:512–516.
13. LaRochelle, W.J., et al. 2001. PDGF-D, a new protease-activated growth factor. *Nat. Cell Biol.* **3**:517–521.
14. Li, X., et al. 2000. PDGF-C is a new protease-activated ligand for the PDGF alpha-receptor. *Nat. Cell Biol.* **2**:302–309.
15. Heldin, C.H., Ostman, A., and Ronnstrand, L. 1998. Signal transduction via platelet-derived growth factor receptors. *Biochim. Biophys. Acta.* **1378**:F79–F113.
16. Rosenkranz, S., and Kazlauskas, A. 1999. Evidence for distinct signaling properties and biological responses induced by the PDGF receptor alpha and beta subtypes. *Growth Factors.* **16**:201–216.
17. Humbert, M., et al. 1998. Platelet-derived growth factor expression in primary pulmonary hypertension: comparison of HIV seropositive and HIV seronegative patients. *Eur. Respir. J.* **11**:554–559.
18. Capdeville, R., Buchdunger, E., Zimmermann, J., and Matter, A. 2002. Glivec (STI571, imatinib), a rationally developed, targeted anticancer drug. *Nat. Rev. Drug Discov.* **1**:493–502.
19. Cohen, M.H., et al. 2002. Approval summary for imatinib mesylate capsules in the treatment of chronic myelogenous leukemia. *Clin. Cancer Res.* **8**:935–942.
20. Dagher, R., et al. 2002. Approval summary: imatinib mesylate in the treatment of metastatic and/or unresectable malignant gastrointestinal stromal tumors. *Clin. Cancer Res.* **8**:3034–3038.
21. Olschewski, H., et al. 2002. Inhaled iloprost for severe pulmonary hypertension. *N. Engl. J. Med.* **347**:322–329.
22. Ghofrani, H.A., et al. 2002. Sildenafil for treatment of lung fibrosis and pulmonary hypertension: a randomised controlled trial. *Lancet.* **360**:895–900.
23. Ghofrani, H.A., et al. 2002. Combination therapy with oral sildenafil and inhaled iloprost for severe pulmonary hypertension. *Ann. Intern. Med.* **136**:515–522.
24. Ghofrani, H.A., et al. 2004. Sildenafil increased exercise capacity during hypoxia at low altitudes and at Mount Everest base camp: a randomized, double-blind, placebo-controlled crossover trial. *Ann. Intern. Med.* **141**:169–177.
25. Zhao, L., et al. 2001. Sildenafil inhibits hypoxia-induced pulmonary hypertension. *Circulation.* **104**:424–428.
26. Eddahibi, S., et al. 2000. Imbalance between platelet vascular endothelial growth factor and platelet-derived growth factor in pulmonary hypertension. Effect of prostacyclin therapy. *Am. J. Respir. Crit. Care Med.* **162**:1493–1499.
27. Tanabe, Y., et al. 2000. Mechanical stretch augments PDGF receptor beta expression and protein tyrosine phosphorylation in pulmonary artery tissue and smooth muscle cells. *Mol. Cell. Biochem.* **215**:103–113.
28. Jankov, R.P., et al. 2005. A role for platelet-derived growth factor beta-receptor in a newborn rat model of endothelin-mediated pulmonary vascular remodeling. *Am. J. Physiol. Lung Cell Mol. Physiol.* **288**:L1162–L1170.
29. Wensel, R., et al. 2002. Assessment of survival in patients with primary pulmonary hypertension: importance of cardiopulmonary exercise testing. *Circulation.* **106**:319–324.
30. Cowan, K.N., et al. 2000. Complete reversal of fatal pulmonary hypertension in rats by a serine elastase inhibitor. *Nat. Med.* **6**:698–702.
31. Nishimura, T., et al. 2002. Simvastatin attenuates smooth muscle neointimal proliferation and pulmonary hypertension in rats. *Am. J. Respir. Crit. Care Med.* **166**:1403–1408.
32. Abe, K., et al. 2004. Long-term treatment with a Rho-kinase inhibitor improves monocrotaline-induced fatal pulmonary hypertension in rats. *Circ. Res.* **94**:385–393.
33. Schermuly, R.T., et al. 2004. Chronic sildenafil treatment inhibits monocrotaline-induced pulmonary hypertension in rats. *Am. J. Respir. Crit. Care Med.* **169**:39–45.
34. Schermuly, R.T., et al. 2004. Antiremodeling effects of iloprost and the dual-selective phosphodiesterase 3/4 inhibitor tolafentrine in chronic experimental pulmonary hypertension. *Circ. Res.* **94**:1101–1108.
35. Jeffery, T.K., and Wanstall, J.C. 2001. Pulmonary vascular remodeling: a target for therapeutic intervention in pulmonary hypertension. *Pharmacol. Ther.* **92**:1–20.
36. Rosenberg, H.C., and Rabinovitch, M. 1988. Endothelial injury and vascular reactivity in monocrotaline pulmonary hypertension. *Am. J. Physiol.* **255**:H1484–H1491.
37. Okada, K., et al. 1997. Pulmonary hemodynamics modify the rat pulmonary artery response to injury. A neointimal model of pulmonary hypertension. *Am. J. Pathol.* **151**:1019–1025.
38. Frisdal, E., et al. 2001. Gelatinase expression in pulmonary arteries during experimental pulmonary hypertension. *Eur. Respir. J.* **18**:838–845.
39. Weissmann, N., et al. 2003. Downregulation of hypoxic vasoconstriction by chronic hypoxia in rabbits: effects of nitric oxide. *Am. J. Physiol. Heart Circ. Physiol.* **284**:H931–H938.
40. Chen, E.Y., Mazure, N.M., Cooper, J.A., and Giaccia, A.J. 2001. Hypoxia activates a platelet-derived growth factor receptor/phosphatidylinositol 3-kinase/Akt pathway that results in glycogen synthase kinase-3 inactivation. *Cancer Res.* **61**:2429–2433.
41. Leppanen, O., et al. 2004. Oral imatinib mesylate (STI571/gleevec) improves the efficacy of local intravascular vascular endothelial growth factor-C gene transfer in reducing neointimal growth in hypercholesterolemic rabbits. *Circulation.* **109**:1140–1146.
42. Van, S.M., Kazlauskas, A., Schreiber, S.L., and Symes, K. 2005. Distinct effectors of platelet-derived growth factor receptor-alpha signaling are required for cell survival during embryogenesis. *Proc. Natl. Acad. Sci. U. S. A.* **102**:8233–8238.
43. Vantler, M., Caglayan, E., Zimmermann, W.H., Baumer, A.T., and Rosenkranz, S. 2005. Systematic evaluation of anti-apoptotic growth factor signaling in vascular smooth muscle cells. Only phosphatidylinositol 3′-kinase is important. *J. Biol. Chem.* **280**:14168–14176.
44. Datta, K., Bellacosa, A., Chan, T.O., and Tsichlis, P.N. 1996. Akt is a direct target of the phosphatidylinositol 3-kinase. Activation by growth factors, v-src and v-Ha-ras, in Sf9 and mammalian cells. *J. Biol. Chem.* **271**:30835–30839.
45. Khwaja, A., Rodriguez-Viciana, P., Wennstrom, S., Warne, P.H., and Downward, J. 1997. Matrix adhe-

sion and Ras transformation both activate a phosphoinositide 3-OH kinase and protein kinase B/Akt cellular survival pathway. *EMBO J.* **16**:2783–2793.

46. Chiorean, M.V., et al. 2004. Imatinib mesylate induces apoptosis in human cholangiocarcinoma cells. *Liver Int.* **24**:687–695.

47. Dan, S., Naito, M., and Tsuruo, T. 1998. Selective induction of apoptosis in Philadelphia chromosome-positive chronic myelogenous leukemia cells by an inhibitor of BCR - ABL tyrosine kinase, CGP 57148. *Cell Death Differ.* **5**:710–715.

48. Cho, A., Graves, J., and Reidy, M.A. 2000. Mitogen-activated protein kinases mediate matrix metalloproteinase-9 expression in vascular smooth muscle cells. *Arterioscler. Thromb. Vasc. Biol.* **20**:2527–2532.

49. Laurent, M., et al. 2003. NOVH increases MMP3 expression and cell migration in glioblastoma cells via a PDGFR-alpha-dependent mechanism. *FASEB J.* **17**:1919–1921.

50. Endo, H., Utani, A., and Shinkai, H. 2003. Activation of p38 MAPK suppresses matrix metalloproteinase-1 gene expression induced by platelet-derived

growth factor. *Arch. Dermatol. Res.* **294**:552–558.

51. Davis, R.J. 1993. The mitogen-activated protein kinase signal transduction pathway. *J. Biol. Chem.* **268**:14553–14556.

52. Sanz-Gonzalez, S.M., Castro, C., Perez, P., and Andres, V. 2004. Role of E2F and ERK1/2 in STI571-mediated smooth muscle cell growth arrest and cyclin A transcriptional repression. *Biochem. Biophys. Res. Commun.* **317**:972–979.

53. Ishizawa, K., et al. 2004. Hepatocyte growth factor induces angiogenesis in injured lungs through mobilizing endothelial progenitor cells. *Biochem. Biophys. Res. Commun.* **324**:276–280.

54. Myllarniemi, M., et al. 1999. Selective tyrosine kinase inhibitor for the platelet-derived growth factor receptor in vitro inhibits smooth muscle cell proliferation after reinjury of arterial intima in vivo. *Cardiovasc. Drugs Ther.* **13**:159–168.

55. Hu, Y., Bock, G., Wick, G., and Xu, Q. 1998. Activation of PDGF receptor alpha in vascular smooth muscle cells by mechanical stress. *FASEB J.* **12**:1135–1142.

56. Resnick, N., et al. 1993. Platelet-derived growth factor B chain promoter contains a cis-acting fluid

shear-stress-responsive element [erratum]. *Proc. Natl. Acad. Sci. U. S. A.* **90**:7908.

57. Buchdunger, E., et al. 1995. Selective inhibition of the platelet-derived growth factor signal transduction pathway by a protein-tyrosine kinase inhibitor of the 2-phenylaminopyrimidine class. *Proc. Natl. Acad. Sci. U. S. A.* **92**:2558–2562.

58. Buchdunger, E., et al. 2000. Abl protein-tyrosine kinase inhibitor STI571 inhibits in vitro signal transduction mediated by c-kit and platelet-derived growth factor receptors. *J. Pharmacol. Exp. Ther.* **295**:139–145.

59. Wilkinson-Berka, J.L., et al. 2004. Inhibition of platelet-derived growth factor promotes pericyte loss and angiogenesis in ischemic retinopathy. *Am. J. Pathol.* **164**:1263–1273.

60. Rose, F., et al. 2002. Hypoxic pulmonary artery fibroblasts trigger proliferation of vascular smooth muscle cells: role of hypoxia-inducible transcription factors. *FASEB J.* **16**:1660–1661.

61. Lowry, O.H., Rosebrough, N.J., Farr, A.L., and Randall, R.J. 1951. Protein measurement with the Folin phenol reagent. *J. Biol. Chem.* **193**:265–275.